CFHTLS-VW Review

L. Allen, J-L. Atteia, M. Boer, T. Contini, J-C. Cuillandre, F. Daigne, A. Doressoundiram, B. Gladman, JJ Kavelaars, A. Klotz, J-P. Kneib, F. Malacrino, F. Mirabel , R. Mochkovitch, J-F. Olive, J.-M. Petit, P. Rousselot, G. Soucail , C. Veillet, Chris Williot

March 18, 2005

Contents

1 The CFHTLS-VW

The CFHT Legacy Survey was designed to bring together multiple science goals that could be effectively achieved using a wide-field imaging camera. The project is intended to achieve a core set of primary science drivers whose scope is beyond that of typical PI mode programs while acquiring a set of observations that will contribute to CFHT's Legacy by providing a dataset of broad utiltiy to astronmers.

2 Science Goals

The CFHTLS-VW was approved as a survey of the approximately 1300 square degrees of the sky within 2 degrees of the ecliptic plane and more than 10 degrees from the galactic plane. The scheduling and execution of the survey is constrained by the primary science goal of a well characterized and unbiased survey of the Kuiper belt. In addition to providing a nearly complete sample of the low-latitude ecliptic plane LS-VW is also being conducted in 3 filters to provide multiple-wavelength information for the entire 1300 square degrees acquired with a scheduling that will provide repeated observations of the same patch of sky at a variety of time intervals adapted to moving-object science.

2.1 The Kuiper Belt

The exploration of the Kuiper belt is the primary science driver for the LS-VW. The observing program balances the need to discover a large number of objects while providing sufficient follow-up observations to allow these primary goals to be met:

- Exploring the stable zones of the outer solar system from 20 to 150 AU
- Measuring the size distribution of the Kuiper belt down to about 100 km
- Providing a homogenous, well-characterized and unbiased sample suitable for modelling the underlying orbital distribution of the belt
- Searching for new orbital classes, as a probe of planetary formation
- Providing a uniformly-derived sample for physical studies

The critical consideration in the design of the survey has been to ensure that the sample of Kuiper belt object (KBO) orbits is 'well characterized' and 'unbiased'. To characterize the survey we carefully measure the detection efficiency as a function of both luminosity and rate of motion. To provide an 'unbiased' survey requires attempting to acquire follow-up observations of all KBOs detected and to avoid selecting follow-up targets based on assumed orbits, heightening the chances of finding 'unique' new objects. These two goals for the LS-VW provide the lever to advance the science of the Kuiper belt. The Kuiper Belt science is exciting because we are still learning first-order things about the Solar System rather than just refining paramater estimates. A more detailed description of the science issues and context of the CFHTLS KBO survey can be found in Appendix A.1.

2.2 Gamma Ray Bursts

The goal of the real time analysis system (hereafter RTAS) is to quickly identify GRB afterglow candidates in the images of the sky recorded as part of the CFHTLS-VW. Using our RTAS we are attempting the first detection of a GRB afterglow directly by optical emission. A detection would certainly have a strong impact on future GRB studies, while no detection would provide significant constraints on the geometry and opening angles of GRB jets. Near real time operation is essential in order to confirm the GRB nature of the detections with follow-up studies while the afterglow candidate is still bright. A detailed description of the GRB science program and the current results of the RTAS can be found in Appendix B.

2.3 QUASARS

Observations of the cosmic microwave background and the most distant quasars have revealed the epoch of reionization and the end of the dark ages. At redshifts between z 15 and z 6 the first sources of ionizing radiation turned on and generated sufficient ionizing photons to reionize the universe. Understanding these early phases of galaxy and black hole formation are key.

Studies of the CMB and quasar spectra provide complementary probes of the reionization history. Temperature and polarization anisotropies of the CMB are most strongly dependent upon the early stages of reionization when the first free electrons appear. Lyman photons, on the other hand, are easily absorbed by even a small fraction of neutral hydrogen, so studies of quasar spectra probe the final stages of reionization.

A search for the brightest QUASARs that may be responsible for the reionization of the Universe is being conducted by extending the LS-VW observations to z'. Further details on the QUASAR project can be found in Appendix C

2.4 Stars and Brown Dwarfs

The VW component of the CFHTLS is also being searched for brown dwarfs, to

- find significantly cooler brown dwarfs than currently known
- identify sufficient numbers of brown dwarf stars to study their spatial distribution and luminosity function
- to better sample the temperature/gravity plane for the 800-1200K T-dwarfs.

The brown dwarf survey will identify several thousand brown dwarfs, and accurately determine their luminosity function in the galactic disc. The large volume probed will also allow the discovery of many ultracool brown dwarfs, and could push the temperature of the coolest known brown dwarfs down by 200 K, at which point the atmospheric models predict a qualitative change in spectra, from methane-dominated (T-dwarfs) to ammonia-dominated (Y-dwarfs).

The main advantages of the VW survey (compared with the Deep and Wide) are the larger sampling volume and brightness of the detected Brown Dwarfs is sufficient for spectroscopic follow-up and characterization. Brown Dwarfs are selected by their red i'-z' colours, since i'-z' is an excellent spectral type estimator for brown dwarfs. This program absolutely needs i' data, for a substantial fraction of the planned coverage of the VW survey and within reasonable delays. z' observations of the Wide are going to be obtained on the Canadian side from PI observations. Further details are available in Appendix D.

3 Survey Status

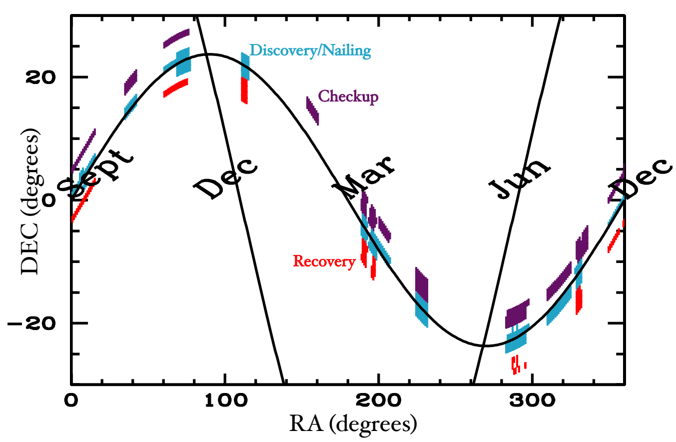

Figure 1: The current area coverage of the LS-VW. The current coverage in each filter is shown by a different color box. g': blue, r': red, i': purple. The i' and r' coverage blocks have been offset +4 and -4 degree in declination to clearly show the coverage in all filters. The months on the plot indicate when that section of sky comes to opposition.

3.1 Observing Strategy

The timing of observations is designed to optimize detection and tracking of Kuiper belt objects. The CFHTLS-VW takes a comprehensive approach to discovery and tracking of TNOs (trans-neptunian obects). During the planning stages of this survey other KBO surveys were beginning to encounter problems trying to track all the objects detected. Careful simulation and examination of previous discovery and tracking campaigns forced us to a plan of Discovery, Nailing, Checkup and Recovery on the LS-VW. After an initial observation of 3 exposures on one night (Discovery) the same patch of sky is re-observed 1 night (Nailing), 6 weeks (Checkup), 1 year (Recovery), and 2-3 (Long-term) later. The LS-VW discovery magnitude limit (g$\sim$24.1) implies about 1 object per square degree we must track before their position uncertainty exceeds about 1800". This ensures that the positional uncertainty in our tracked KBOs never lead to confusion between objects, provides a high likelihood of re-locating previously discovered objects and lowers orbital uncertainty with a minimum set of observations. Figure 2 demonstrates the evolution in orbital and position uncertainty for one of the TNOs discovered in the LS-VW pre-survey begun in 2002 to test the observing strategy. As of November 2004, 50 LS-VW objects (those few discovered in the shaky survey start-up phase before November 2003) had reached the point of Recovery. Even after 1 year of tracking the orbit uncertainty is ∼3 AU, useless for resonance mapping or long term dynamical studies. However, at the 2nd-Year observation (summer 2005) the uncertainty will be driven below about 0.1 AU. More details on the observing strategy can be found in Appendix A.3

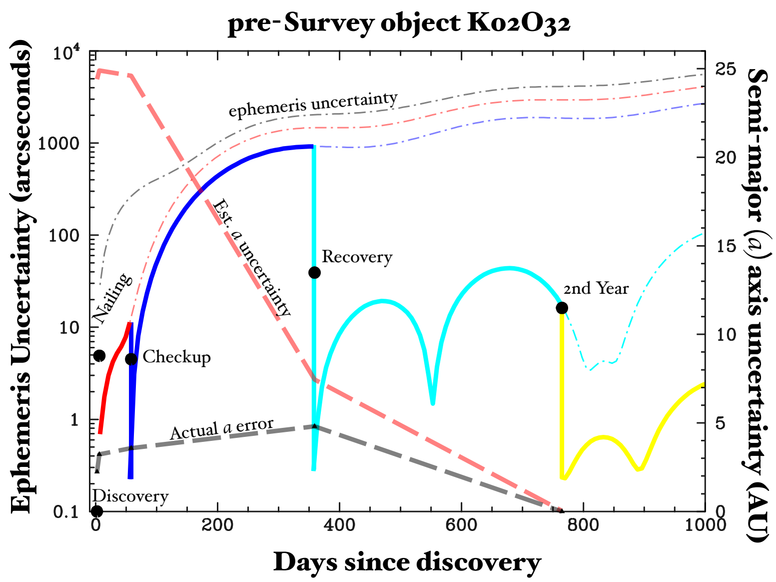

Figure 2: Evolution of orbital and ephemeris uncertainty within the LS-VW. K02O32 is an object discovered in the CFEPS pre-Survey and tracked using the strategy developed for the LS-VW. Discovered in the summer of 2002 K02O32 has now been tracked for about 780 days, and is thus a 'final' orbit. The SOLID lines track the evolution of the ephemeris uncertainty [left axis, in arcsec]. The dot-dashed lines indicate how the ephemeris uncertainty would evolve if a particular observation (Nailing, Checkup, Recovery, 2nd Year) were missed. The thick-dashed line indicates the evolution of the semi-major axis (a) [right axis, in AU] with each observation, red is the formal error and black the actual error compared to the final elements; in this case the best estimate was always within 1 AU, which is not always the case as shown in the appendix.

3.2 Area Coverage

The progress of field coverage the LS-VW is measured by 3 linked observations (which are usually multiple exposures) of the same field, called Discovery, Nailing and Checkup. Each of these 3 observations represents acquisition of a new filter and a new epoch. They provide the critical time sampling needed to build a robust detection of TNOs and they satisfy the first phase of the LEGACY aspect of the observations (multiple filters). As of December 2004 approximately 250 square degrees has been observing in this way. The survey is now beginning the 3rd year of operation and 'Long-arc' proper motion observations have not yet been made of any of our fields. The goal of the project is to provide observations of 1300 square degrees of sky. The present rate of new field acquisition (Discovery, Nailing and Checkup) minus the time needed to begin Long-arc proper motion observations, will result in a total area coverage of approximately 600 square degrees (about 1/2 of the target coverage). The priority assignments within the LS surveys has ensured (and will continue to ensure) that nearly all fields which received Discovery observations will also be observed at the Checkup and then Recovery epoch. Approximately 3 years after the initial observation of a field a final set of Long-arc images is intended be taken to allow the detection of proper-motion of galactic field stars and to provide the final astrometric measurements needed to secure the orbits of the LS KBOs. At the time of this report (March 15, 2005) no fields have a base line of more than 2 years, thus we have not yet made any Long-arc observations. In the LS-VW pre-Survey we used a base line of 2 years from discovery for TNO orbit determination, which is sufficient for the TNO science. However, 2 years was deemed too short to allow stellar proper motions and thus the baseline was extended to 3 years to allow stellar proper motion measurements.

3.3 Filter Coverage

The goals of the primary science case do not require observing in different filters at the different epochs (see Figure 1). To enhance the opportunities for additional science use of the LS-VW data the Discovery, Checkup and Recovery observations are each made in a separate bandpass (g', i' and r'). The final Long-arc observations will then be made in the same filter as the discovery pass (usually g'). Owing to the required time sequencing and the linking of filters to timing, each patch of the sky acquired as part of the LS-VW has g',i',r' observations made within about 1 year of the first observation of the field, providing 3-colour data within one year. Roughly 300 square degrees of sky is already available in multiple filters, with summed limits of roughly 24th magnitude (depending on seeing and filter).

3.4 Image Quality and Depth

Image Quality The majority of frames acquired for the CFHTLS-VW have had image quality measurements better than that of the original survey plan. After the first few months of the survey the Discovery exposures were shortened to ensure that objects Discovered in g' could be effectively followed at Checkup using short (3 minute) i' exposures. Because of the severe time constraints at Checkup (the observation window during which Checkup observations are possible is typically only 6 nights, and the observations must occupy the first 3 hours of the night) the image-quality constraints on these exposures has been looser than for g'. Overall, the majority of data acquired has image quality that is sufficient for TNO detection and tracking.

Photometry The majority of data acquired for the Discovery epoch (almost all in g') has been done during photometric conditions. During the Checkup observations time-constraint issues result in a small number of exposures been made in non-photometric conditions. These non-photometric images will be calibrated using overlapping fields from the USNO and SSDS catalogues.

Time Criticality The LS-VW has strict timing constraints that are in partial conflict with the QSO model. However, the flexibility of QSO observing has been critical to ensuring that observations are made when the time constraints and weather requirements allow; CFHT has been doing a good job with this. 256 of the 288 square degrees covered at a discovery epoch (the observation which then triggers a set of time-constrained observations) have also had the required Checkup observation made. This rate of successfully re-acquiring fields is remarkable and would be impossible in a classically scheduled environment. The two lost blocks (a block is about 16 contiguous square degrees) were the result of the very bad weather and camera failure in February 2004.

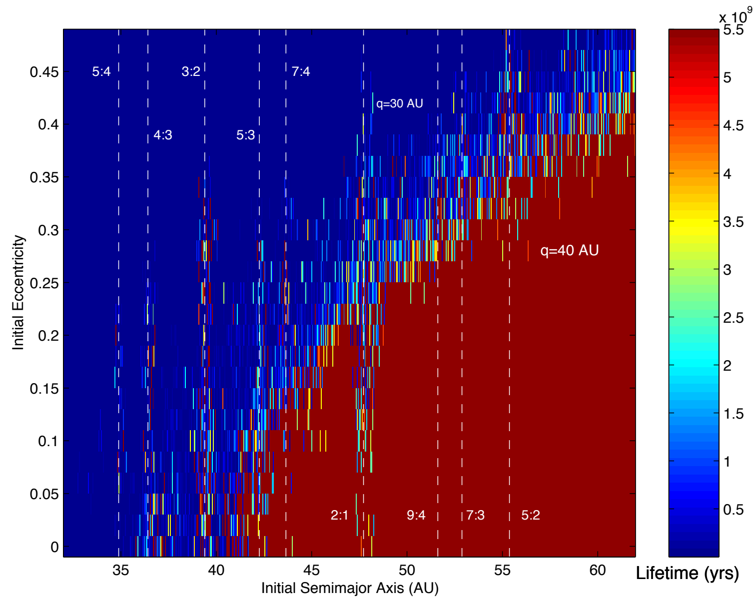

Figure 3: The figure shows a calculation of the orbital stability time for the outer Solar System outside Neptune. Objects were placed on a grid of initial orbits; this diagram shows the initial $i = 11^{\odot}$ slice. Burgundy areas are stable; in other figures in this document the colour table will be converted to a greyscale (white stable). Various mean-motion resonances with Neptune are marked with vertical bars. Note in particular the following features: (a) the main belt outside about 41 AU, (b) the fingers of stability at high-e due to the orbital resonances for objects with the correct resonant angles (combination of phases), (c) regions of instability descending into the stable regions.

All images acquired for the CFHLS-VW have met or exceeded the standards required for the KBO project to be successful.

4 Science Exploitation

4.1 KBO Science: The Canada-France Ecliptic Plane Survey

CFEPS is the banner under-which the Canadian and French Kuiper-belt community members participating in the CFHTLS-VW have organized. This project includes 6 full-time researchers, 3 postdocs and 3 graduate students, as well as several scientists outside the Canada-France community.

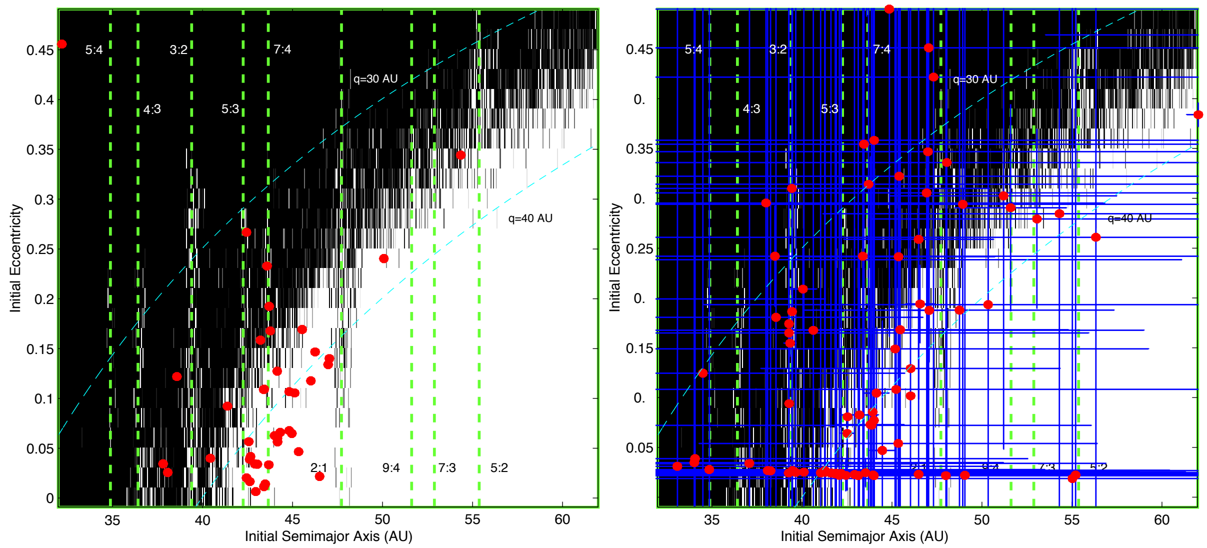

Figure 4: The same stability region as in Fig. 3 but with orbital stability converted to a greyscale, and with the orbits of the VW pre-Survey KBOs [left panel] and CFEPS KBOs [right panel] overlain. The VW pre-Survey objects have observed arcs of at least 2 years duration (that is, seen on three different oppositions). Such objects with well-determined orbits and can be used as probes of the dynamical sub-components of the belt. The CFEPS objects will have similarly well determined orbits once their Long-arc observations have been acquired. As the number of secure orbits increases zones of stability that are NOT occupied become increasingly interesting as markers of some unknown perturbation or primordial process. However, there are still *very strong* detection biases towards nearby objects which make the discovery of low-pericenter objects (for example) much more likely (making it more likely to find objects which 'hug' the inner edge of the stability region near the perihelion q=40 AU curve). Without knowing the correct characterization of the detections and with heavily-biased orbit samples, incorrect and misleading conclusion can be drawn. **Option B for saving time in the LS-VW requires that additional telescope time [outside the LS-VW] be acquired to achieve these highly precise orbits.**

4.1.1 Initial Orbits

To meet the requirement of 3 years of tracking, to establish good orbits, and to deliver science as quickly as possible, the LS-VW project began near the start of semester 03A. During the initial survey startup the pressure to acquire new fields and track those new objects resulted in some observations being made in less then ideal conditions. However, as of Dec. 2004 LS-VW has discovered, tracked (for various arc lengths, depending on discovery date) and characterized the discovery data for a sample of about 120 TNOs. This sample represents the largest tracked and characterized sample of KBOs currently available, although the precise orbits will not begin to flow until mid-2005. Figures 3 and 4 demonstrates our samples in relation to a stability calculation of the region of the inner part of the Kuiper Belt. The improvement in the coming year will be dramatic as can be attested to by examining the pre-survey objects.

4.2 First Results

The inclination and distance measurements at discovery can be more robustly determined than the semi-major axis and eccentricity and are thus good candidates for first science results. Figure 5 presents the inclination distribution for all CFEPS (LS-VW) KBOs with arcs longer than 2 hours [determining inclination requires a minimum 24 hr arc] along with the inclination distribution for KBOs discovered near the ecliptic pane, as currently listed in the Minor Planet Center orbit database (http://cfa-www.harvard.edu/iau/mpc.html). The CFEPS objects exhibit a more extended inclination distribution than the MPC objects [a KS test gives a probability of $\sim 3\%$ that these to inclination distributions come from the same underlying distribution. This results indicates that the Kuiper belt is more extended than was previously thought. Already modelers are having difficulty producing the high inclination component of the Kuiper belt, clearly the problem is even more difficult then was previously known.

Brown (2001, ApJ, 121, 2804) suggests a two component model of the inclination distribution, based on the MPC database. Using this first CFEPS inclination result (Figure 5) we can now reject this model (Kavelaars et al. *inprep*) at the 97% level. To improve this result and demonstrate that the observed Kuiper belt is now a two component system will require a minimum of 4 time the number of detections as in the current CFEPS db.

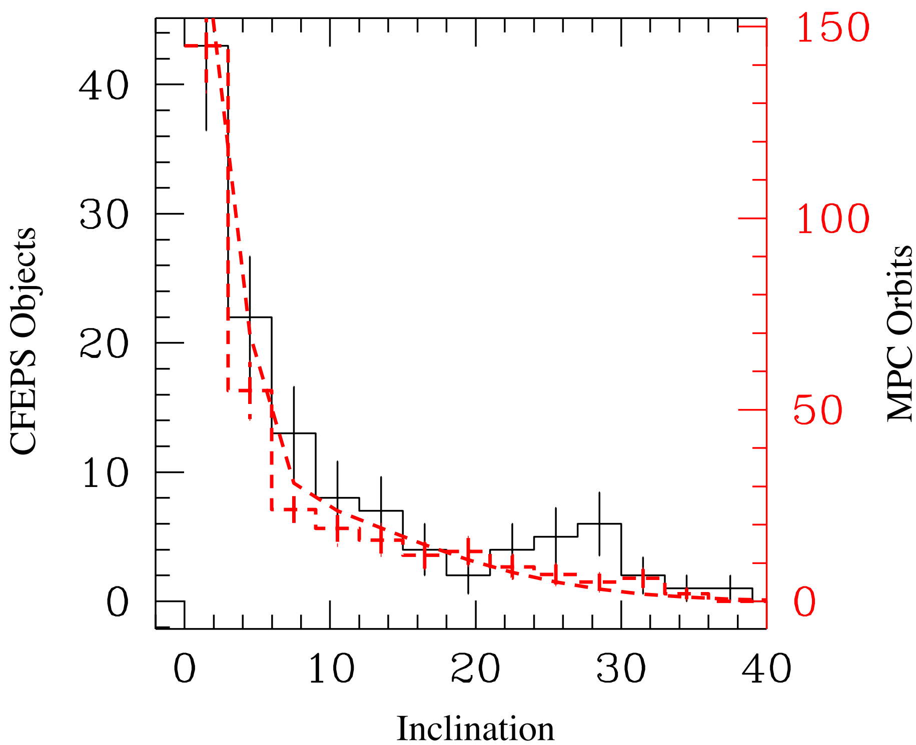

Figure 5: The distribution of orbit inclinations for KBOs discovered by CFEPS (black line) and as currently listed in the MPC. The red histogram points (with error bars) is the observed MPC objects that were discovered within 2 degrees of the ecliptic. The red smooth curve is the model fit from Brown (2001). A KS-test gives a 3% chances that MPC db (or Brown's model) and the CFEPS db come from the same parent population. The most likely explanation is that previously unknown biases are affecting the MPC inclination distribution. [Brown's model, as shown, already accounts for the bias towards low-i orbits when observing near the ecliptic]

Planet formation scenarios are very effectively ruled out or accepted via comparison with a well describe set of observational test. For too long, the Kuiper belt has lacked such a data set. In addition to providing the required dataset, CFEPS is also producing a 'Survey Simulator' that will be publicly available and will allow modelers to directly compare their model the CFEPS db Bench Mark. Our goal is to become the gold standard of KBO orbit databases. The use of the Survey Simulator to compare observations to models is described using the MPC as an example in Appendix A.4.

5 Future of the LS-VW

The original goal the CFHTLS-VW was to cover the entire 1300 square degrees of search area twice (Discovery/Nailing and Checkup) during a 6-year span. Began in May 2003 the CFHTLS-VW has now been running for almost 2 years and should have covered about 800 square degrees of sky, but has instead managed to cover only 288 square degrees. The major delay has been caused by the combination of exceptionally poor weather on Mauna Kea and the technical problems typical of any new instrument (exacerbated by the enormous complexity of MegaPrime). Because of the time critical nature of the CFHTLS-VW observations and those of the SNLS project, meeting both sets during these poor conditions was impossible and attempting to do so would hobble both projects. Thus, at the recommendation of the CFHT SAC, the SNLS project was given priority and the LS-VW and Wide components of the survey ran at 'half speed' during this time period.

As a result of the slow data rate the KBO science team recognized that the sky covered *would not be contiguous enough* to allow tracking of KBOs if the baseline between return visits exceeded 1 year. The TNOs would exit the Legacy Field patches, yielding loss of more than half the objects. Thus, in 2004A, a strategy of re-observing the LS-VW fields at 1-year epochs was adopted. However with this additional load the amount of area covered by the survey is about 50% that which could be anticipated if the CFHT MegaPrime was able to deliver 6.5hrs of Open Shutter time per night. Running at 50% speed is creating the risk that LS-VW will become noncompetitive, particularly in light of Pan-Starrs commencing operation in January 2006 and the looming Discovery Channel Telescope, scheduled for completion in 2009. How can the KBO science program maintain its competitive edge without compromising the other science goals of the LS-VW? To ensure success to the project, the CFHTLS-VW must configure itself to achieve the KBO sequencing at a competitive rate of discovery using only 70% of the time allocated to it (ie. the time that will actually be achieved) OR the SAC/Board must recognize the short falls inherent in the current time budget and allocate an additional 30% observing time to this component of the project.

5.1 A Plan for the Very Wide

5.2 A plan for the Very Wide

Here we describe possible scenarios for reallocating the LS-VW exposure time to allow the KBO program to proceed in a more competitive manor. Table 1 presents the current cost, in seconds, for each square degree of LS-VW observations. [Descriptions of the circumstance terms are provided in Appendix A.3. Table 1 presents 2 options for changing the sequencing of the LS-VW in order to ensure the core KBO science is achieved in a timely manner.

	Current				Option A				Option B			
Type	filter	nobs	itime	Cost	filter	nobs	itime	Cost	filter	nobs	itime	Cost
Discovery	g’	3	80	360	g’	3	80	360	g’	3	80	360
Nailing	g’	1	90	90	g’	1	90	130	g’	1	90	130
Checkup	i’	3	180	660	r’	3	110	450	i’	3	180	660
1 year	r’	4	110	600	g’	4	90	520	r’	4	110	600
3 year	g’	4	90	520	g’	3	90	520		Delayed		
Sub-Total				2270				1980				1750
i-Band					i’	2	270	620				
+3 years									g’	3	90	520
Total				2270				2600				2270

Table 1: **Current:** Integration time in seconds for a single LS-VW field. The ’Cost’ column is the amount of time, including the 40s overhead charge, for all the exposures of given circumstance. This sequence costs 2270 seconds per field and provides full filter coverage and a 3 year baseline for proper-motion followup. **Option A:** Discontinue observing the ’Checkup’ (see Appendix A.3) in i’ and switch to r’, pushing the i’ observations to later in the survey and in B-queue. This option effectively delays the i’ filter until 2007 or 2008. This option reduces the cost of a single field for KBO science to 1980 seconds from 2270 (a savings of 13% and thus allows 13% more area to be covered. The i’ observations would be placed into the B-queue and executed if time permitted. Once the KBO survey is completed (in 2008A) the i’ observations would be done a full speed. This option is not sufficient to make up the entire 30% short-fall. **Option B:** Delay the 3yr follow-up epoch until after 2008. This provides a longer baseline for stellar proper-motions. *Plan B requires that a substantial recovery program at another 4+meter facility be available, making the KBO project dependent on external [non-CFHT] resources.* This plan would save about 23% of the observing time during the critical KBO discovery sequence however, the saving would not be realized until the first fields come to their 3rd recovery observation in 2006B (see Table 2).

5.2.1 Option C

Some combination of B and A together. By initially placing the i’ observations into the B-band of LS-VW the discovery rate of KBOs can be immediately accelerated and by then delaying the 3 year followup to 2007, a saving of 30% per field can be achieved. Once the KBO project has achieved a satisfactory level of coverage ($\sim$ 800 square degrees) then the filter sequencing and 3 year follow-up can be ramped up and the discovery rate of KBOs ramped down. This option has the best chance at ensure the success of the KBO project while, in the long term, satisfying all the needs of the other science components. Table 2 describes the rates at which new fields would be acquired under various options. The main goal of this plan is provide a mechanism for the mutli-filter long baseline nature of LS-VW to not impede the KBO science when the observing conditions are sub-optimal, as has been the case for the last 2 years on Mauna Kea.

	40hrs A band + 0hrs B band					50hrs A band + 20hrs B band				
	Original		Option C			Original		Option C.		
Semester	DNC	3yr	DNC	i-band	+3yr	DNC	3yr	DNC	i-band	+3yr
05B	87	0	112	0	0	181	0	151	116	0
06A	63	45	109	0	0	108	45	95	116	0
06B	55	56	91	0	0	100	56	108	116	0
07A	53	87	93	0	0	123	87	139	116	0
07B	0	74	70	50	0	0	74	117	138	0
08A	0	80	0	154	0	0	174	0	7	0
08B	0	87	0	2	242	0	181	0	0	281
09A	0	63	0	105	179	0	108	0	0	266
09B	0	55	0	118	161	0	100	0	0	225
10A	0	53	0	47	234	0	123	0	0	273
03A=05A			342					436		
Total	599	599	817	817	817	947	947	1045		1045

Table 2: The likely coverage of LS-VW using the currently approved observing strategy, covering i' at the same rate as g' and r' and returning for proper-motion followup after a 3yr delay versus Option C outlined in the text. 2 scenarios are outlined, one in which the survey operates at 40hrs of A-band per semester (typical of the current rate) and one in which 50-hrs of A-band and 20-hrs of B-band are executed per semester [the full allocation]. In the poor weather (40hr) case Option C results in 30% more coverage than current strategy. In the good weather (50+20 hrs) case Option C results in 17% more coverage than current strategy and i-band is acquired at a rate of +100 square degrees per semester.

Appendices

A Details on the KBO project

A.1 Questions in Planet Formation

The Kuiper Belt is not the cold quiet place which many expected. Instead, we have found a dynamically excited, heavily depleted belt of material. Numerous questions have sprung from this discovery:

- What caused the dynamical excitation in the belt? Current suggestions include: a close stellar passage, the scattering of lunar sized bodies from the inner solar system into this region or the scattering of a nascent Neptune into the region. Each of these scenarios, and others, provides a unique signature in the orbital dynamics of the region. Only an extensive catalog of orbital information will reveal the truth.
- Can objects form in the region beyond 50AU? Currently there are no objects on circular orbits beyond 50AU from the Sun. Why? Again a number of explanations have been proposed. Perhaps a close stellar encounter would truncate the disk at some radius. Perhaps the Sun was born in a nursery of stars and photo-evaporation removed much of the material. Additionally, recent modeling suggests that the actual process of dust accretion and growth may not function on rapid enough time scale in this region. A survey covering a wide area of the ecliptic will allow the detection of the apparently rare objects in this region of the solar system.
- What is the size distribution of material? Crucial to understanding the processes of dust accretion and planetesimal growth is a measure of the actual *size distribution* of large planetesimals (100-500km) in the Belt. Are these objects distributed in a "cascade" of sizes, caused by the competing effects of accretion and erosion or, is the distribution of sizes indicative of only one of these processes. The Belt is now known to contain multiple components and there is growing evidence that these components possess unique size distributions. Our modelling is showing that the size distribution not only affects the 'luminosity function' of the belt but has a very strong effect on the detected orbital distribution.
- What are the largest members of the belt? Tombaugh's discovery of Pluto was aided by Pluto's close approach. However, there is now reason to expect that Pluto is not the most massive member of this region. A comprehensive and complete survey has a chance to determine the largest member of the population and thus further guide our understanding of planetesimal accretion.

In addition to these questions new ones will undoubtedly arise. The exciting thing about this science is that we are still learning first-order things about the Kuiper Belt that are having major ramifications on our understanding about the current structure and past evolution/formation of the outer Solar System. Examples are the discoveries of objects in the Extended Scattered Disk like 2000 CR105 (Gladman et al 2002) or Sedna (Brown et al 2004), or new resonant classes like the 5:2 (Chiang et al 2003). This science is thus NOT improving parameters by 20% but rather discovering the base structure of our Solar System. Our lack of knowledge of the full content of this region severely constrains our understanding of our giant planet formation. Only a large scale survey of the region can solve these riddles.

A.2 Other KBO surveys

A number of competing surveys are either currently operating, have recently finished or will soon be starting. Pan Starrs begins operation in 2006 and all the LS-VW projects must make significant progress within the next year to maintain the potential created by the lead which CFHT gained when it deployed Megacam as the first degree-field camera on a 4-meter class telescope. At the present only two KBO projects relevant to the CFEPS project are underway or completed.

- The KPNO Deep Ecliptic Survey has recently completed a survey resulting in the detection of some 400 KBOs and tracking of about 250 of those objects. However the DES project is *not well characterized* since its magnitude efficiency is unknown. Because the initial survey had only minor tracking resources the orbit distribution may be *highly biased*, or at least these biases cannot be modelled because of the unknown magnitude-dependent efficiency. As a result, using the DES orbits to measure structure in the outer solar system suffers many of the pitfalls that using the MPC database does [see Figure 5].The careful tracking and characterization of the CFEPS project is already yielding much stronger statements to be made about the structure of the Kuiper belt.
- A survey for bright ($m_R < 20$) KBOs is currently underway at the Palomar Observatory Schmidt telescope. This project is complementary to the CFEPS project, covering about 10000 square degrees but only be sensitive to the brightest 100 KBOs. Although the 100 objects will be *interesting for physical studies* (because of their brightness) the orbital database will be an order of magnitude too sparse to allow careful discrimination between planet formation scenarios that imprint differing signatures on the belt.

A.3 Observational Timing Strategy

As mentioned in the main text, the timing of these observations is designed to optimize detection and tracking of Kuiper belt objects. Tracking as many objects as possible while maintaining a bias-free sample is vitally important. The orbital properties of KBOs derived from the CFEPS will be a major improvement over any other data set currently available and will enable a proper comparison with dynamical model predictions.

The basic observational timing strategy for each CFHLS-VW field is as follows :

1. Discovery — a set of 3 short images of the field, each separated by about an hour. This triplet of images is used to discover the KBOs in the field. Three images are necessary to allow automatic pipeline detection of the moving objects. With only two images, the number of false alarms is too high, as noise variations or centroiding errors can easily mimic the potential motion vectors of our KBO targets. Three images within one night reduce the possibility of these noise variations matching the KBO motions, making the number of false alarms manageable.
2. Nailing — a single image of each field obtained within four nights (either prior or after) the discovery triplet. Ideally this nailing image is taken within one night of the discovery triplet, but weather does not always allow this. Experience has shown that waiting more than four days is problematic, as it is extremely difficult to locate the moving objects and many objects shear off the field of view. The

nailing image allows a better determination of an objects motion and definitively separates asteroids from KBOs.

3. Checkup — a second triplet of images two months, taken either two months before or two months after the discovery triplet. This set of three exposures is once again taken with about an hour separating each image. The checkup images allow the determination of the orbit of the KBO well enough that it can be recovered one year later.

4. Recovery — this is a repeat of the discovery triplet and nailing sequence. This observation is what allows the KBO to be recovered in the following few years. After this observation, the second year recovery positional error ellipse is generally less than $30''$. However, without this observation, the KBO cannot be later re-observed and linked back to the discovery object with any confidence.

5. Long-arc recovery — at present this is planned to be completed at three years after discovery. It is basically a repeat of the first year recovery. This observation allows a measurement of the KBO semi-major axis, eccentricity, inclination, mean anomaly, longitude of node, and argument of perihelion adequate to serve as a constraint on dynamical models. Without this measurement, the error on the orbit is too large to allow for details in the models, such as classification into resonant and nonresonant objects.

The discovery images are conducted when the target fields are at opposition. This makes discrimination between KBOs and asteroids possible, although not absolute without the nailing image. Each discovery triplet is part of a group of about 16 fields, which are observed together throughout the rest of the observational sequence and named a Block. By grouping the fields into blocks, we can cycle through each field in the block every time they are observed i.e. for the discovery triplet, one image of each of the 16 fields is taken, then a second image of each of the 16, and so on. This allows a natural spacing of approximately an hour between each exposure of the same field. This same grouping is preserved for checkup and recovery, for the same reason.

The timing of each subsequent astrometric observation is a balance between uncertainty in the position of the KBO and uncertainty in the orbital parameters. Waiting for longer periods between observing an object makes the astrometric measurement more valuable for reducing the uncertainty in the orbital parameters, but waiting too long allows the uncertainty in ephemeris to become larger, thus risking losing the object. This balance is illustrated by some examples of KBOs we have discovered and tracked previous to the CFEPS project (see Figures 6). The orbital parameters and ephemeris uncertainties are calculated using the software distributed by Bernstein & Khushalani (2000).

The first observation after the discovery triplet is nailing. The nailing observation is not strictly necessary in order to find the KBO again two months later, as the positional error by that time may only grow to $\approx 100''$. However, with only the discovery triplet and a checkup triplet two months later, the error in the ephemeris will then grow beyond one degree by the one-year recovery observations, at which point the object could be considered "lost". This can be seen in Figure 6, where the ephemeris uncertainty of one of our typical objects, K02P12, is plotted in panels (c) and (d). By adding a nailing observation, as for K02O32 in panels (a) and (b), the error remains below one degree at the one-year mark. Since we expect KBOs to have a spatial density of approximately one per square degree at the magnitude level of this survey, a positional error of less than one degree is desirable for accurately linking moving objects.

While the discovery images are taken at opposition, the checkup observations could be conducted at any

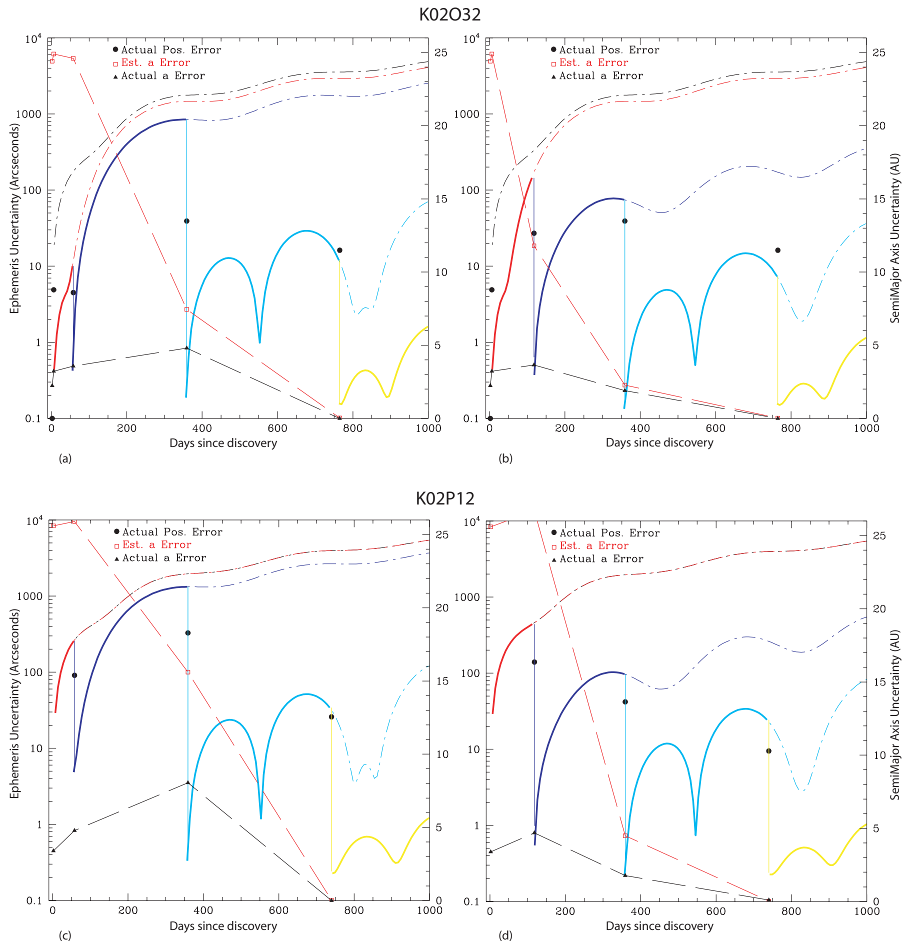

Figure 6: Evolution of positional uncertainty and orbital uncertainty with time, for two typical KBOs. K02O32 and K02P12 are KBOs discovered in our CFEPS presurvey, each of which was tracked for a two year period. These plots illustrate different tracking strategies. K02O32 and K02P12 have slightly different orbits, are both generally circular, low-inclination, low-eccentricity objects typical of "classical belt" KBOs. Panel (a) shows an ideal tracking pattern of discovery, nailing, two-month checkup, with one and two year recovery. Panel (c) shows the same thing, but without the nailing observation as K02P12 was not visible in the nailing image. Panel (b) and (d) show the evolution of uncertainties if the objects are followed up at 4 months instead of 2. Notice that the positional uncertainty grows to greater than a degree if nailing or checkup is not obtained within one year, meaning the object becomes "lost". The timing of observations balances the risk of losing an object and obtaining the best limits on the orbital positions, subject to practical considerations like queue programming and evening visibility.

time in the next four months before the objects disappear behind the sun. Waiting until the end of this four month period means the estimated error in the TNO position is an order of magnitude higher than it would be two months after opposition. If an object was missed in the nailing image due to a chip gap, bright star, TNO shear or brightness variations, a two month wait until checkup may be all that is possible before the error reaches one degree and the object is lost. However, waiting provides the best limits on positional uncertainty for future observations, potentially reducing the error to below $100''$. It does even better at reducing the error in the orbital parameters. With a checkup observation at four months rather than two months after opposition, the error in semi-major axis is reduced by an order of magnitude after the one-year recovery observations are taken. This is illustrated in the comparison of panels (a) and (b) or (c) and (d) of Figure 6. With a confirmed nailing image and the ability to do a target-pointed recovery observation, a four-month period after discovery and nailing before the checkup observation would be optimal.

However, for CFEPS, the checkup images will not be targeted recoveries, but rather a re-imaging of the initial discovery pointings, taken using the same queue process as the original discovery triplets. This is due to the nature of the Legacy Survey. Waiting until four months after opposition then becomes impractical. Because the KBOs are moving very slowly through the sky this far from opposition, the motion is undetectable on a single night and images would have to be taken on successive nights. As fields are not searched by eye but rather by software, linear motion of the KBO between frames is required, and four months after opposition, the motion is nonlinear between successive nights. More importantly (as the previous problem could be dealt with, although at considerable human effort), the observations become almost impossible to schedule into the queue due to time constraints such as the field setting right at the start of the night and requiring good weather on three successive nights. Waiting to three months after opposition gives some gains in the orbital parameter errors after one year also, but there are similar time constraints related to the field being available for only a short time at the start of the night and TNOs are nearly stationay at this time. Therefore, due to practical considerations outside the orbital determination, the checkup observations are conducted two months after opposition.

One year recovery observations are again taken near opposition to avoid asteroid confusion and to allow for efficienct identification of the TNOs. A two-month deviation from this timing, such as would be possible within the queue, does not make much of a difference towards reducing uncertainty in semi-major axis or positional error, but would make detecting the KBOs much more challenging. The one-year recovery observation reduces future positional uncertainty to the order of an arcminute, allowing for easy future observation of objects. However, with only a two-month baseline baseline between discovery and checkup, the semi-major axis uncertainty is still between 1 and 10 AUs after only one year. A further observation at two years is required to reduce the orbital parameter uncertainties another order of magnitude, to the levels necessary for dynamical modeling or resonance family determination.

The necessity of following each KBO for at least two years before measuring orbital parameters can be illustrated here with the small sample of 9 KBOs from the CFEPS presurvey. These 9 objects were followed for two years after discovery. Unfortunately, in this small sample, only a limited sub-population of the Kuiper belt is represented — these are all "classical KBOs", having low eccentricities and inclinations, and semi-major axes between 40 and 50 AU. As a result, the error ellipses on many of the measured quantities (distance, semi-major axis, etc.) appear larger than the final scatter in the actual measurements. This is due to the assumptions allowed into the orbit-fitting code: the best-guess orbit turns out to be generally correct in these low-e, low-i cases, but other (perfectly reasonable, physically possible) orbits cannot be ruled out from the initial observations. It should be noted that these best-guess orbits are not always correct

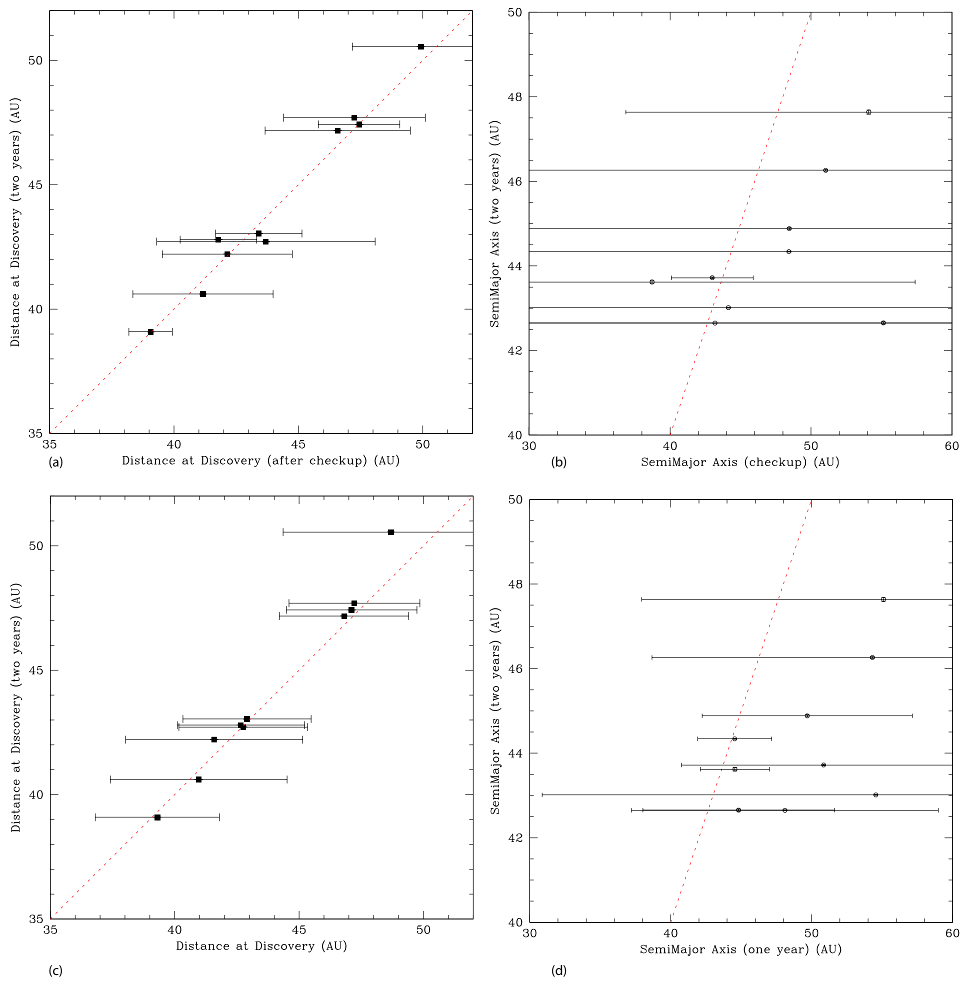

Figure 7: Estimates of the barycentric distance and semi-major axis at checkup vs. the same quantities measure after two year recovery, for our CFEPS presurvey sample. The distance, although it has large errors after only discovery and nailing, is generally accurate enough to work with at this point. The semi-major axis is not very accurately measured after checkup, and instead requires at least a two year observational arc when observed on the CFEPS schedule before uncertainties are reliably low. The estimated semimajor axes tend to be initially above the true value due to assumptions in the orbit-fitting code, especially for this sample. At checkup, the line of sight velocity is so poorly determined that the code assumes a value: after one year, this constraint is relaxed and the code assumes an orbit near perihelion to fit the astrometric measurements. After two years, the line of sight velocity can be measured much more accurately and a “final” orbit can be determined. There are still error bars on each of the data points in the distance and semi-major axis distribution at two years, but they are smaller than the data points.

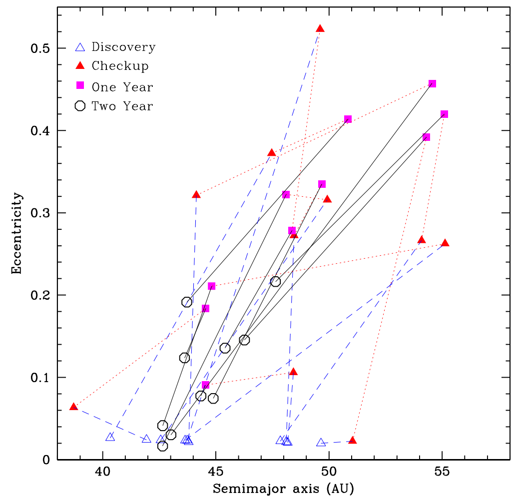

Figure 8: Semi-major axis vs. eccentricity for 10 objects from the CFEPS presurvey, as measured at discovery (open triangles), checkup (solid triangles), one year recovery (solid squares) and two year recovery (open circles). Semi-major axis and eccentricity are important parameters for determining the classification of a KBO, including possible resonance with Neptune.

and following the assumptions alone would preclude discovery of new and special dynamical classes, such as the "extended scattered disk" objects. It would also lead to a biased view of the dynamical state of the Kuiper belt, as new objects would only manage to be re-observed (rather than lost) if they fit the previous assumptions on the orbital classification.

What becomes clear in looking at Figure 7 is that some basic parameters, such as the distance of each KBO, may be determined relatively reliably as early as the nailing image. However, the semi-major axis and other orbital parameters are very poorly measured until two or more years of total orbital arc are available. The uncertainty in orbital parameters can be seen in a different manner in Figure 8, where the semi-major axis and eccentricity are plotted for each object at different points in the orbit-refinement process. While the distance distribution can be interesting as a first-order test of models of the Kuiper belt (for example, the question of a Kuiper cliff at 50 AU can begin to be tested using the distance distribution), we have come to understand that the Kuiper belt is much more complicated than a simple radial distribution. Knowledge of the complex multi-dimensional orbital parameter distribution is necessary in order to test present dynamical models, such as stellar close encounters, migrating giant planets, or scattered planetary embryos.

A.4 Modeling the Kuiper Belt: First CFEPS results

Figure 4 shows how dramatically orbits improve once observations two or more years of arc in baseline are acquired. It is obvious that with the 2-day to 1-year arcs of the CFEPS objects which have now been obtained since the start of the survey (depending on how long ago the Dicovery epoch observations were obtained) the orbits are still highly uncertain and very little can be said about the real orbital distribution. But the survey strategy is built around the realization that 2-year or longer arcs are required to specify the orbits. Fig. 4 also showed a set of well-characterized and long-arc (2 years or more) orbits from previous CFHT data including the CFEPS pre-survey from 2002. The orbit improvement is dramatic, and we can then proceed to actually model the 'real' (unbiased by the flux limits and tracking bias of the survey) underlying orbital distribution. We can do this because the pre-surveys, like CFEPS, are well-characterized.

We can then apply a simulation of the survey, knowing the areal coverage, magnitude and rate efficiency of the survey, for every patch of observations. It is critical to point out that this has never been possible for a large survey in the field of Kuiper Belt science. We are publishing the survey simulator as a progressively increasing sample of observing fields, their survey parameters, and a list of detected objects.

A.4.1 Distance distribution

As a simple example, let us examine the question of an outer Kuiper Belt edge; a topic frequently addressed in the literature. Previous studies by Allen et al (2001) and Trujillo & Brown (2001) indicate there exists a cutoff in the radial distribution between 45 and 50 AU. An actual quantification of the error in the location of this cutoff is difficult, and if the size distribution of objects changes with distance, neither of these analyses are accurate.

Let us consider the application of a very simple model to our survey simulator. The underlying distribution is such that the stable phase space (Fig. 3 is full, convolved with a decaying power-law in the surface number density with increasing semi-major axis to give a reasonable initial protosolar disk. We then truncate this simple model at either the 2:1 resonance at 48.4 AU or continue it out to 100 AU (beyond which we would only detect rare objects larger than 1000 km in diameter). How reliably can we determine which of this rather different models is better supported by the available data?

Applying the survey simulator to this model distrbituion, Figure 9 shows that we would expect to see a dropoff in the number of objects detected beyond 45 AU in both models. If a cutoff at 48.4 AU was present (the stable objects have non-zero eccentricities and thus extend out further from then Sun when at aphelion) then almost no obects are seen past 55 AU. However, the lever arm available to distinguish between these two models is a shockingly-low fraction of the detected TNOs, due to the extreme flux bias caused by both the reflected light and the steep Kuiper Belt size distribution favoring detection at smaller distances. In fact, while the LS-VW transneptunian object distance distribution appears significantly different than the available Minor Planet Center (MPC) database (K-S probability of 4 percent that the LS-VW detections come from the same distribution), whether there is an outer edge to the Kuiper belt can only be verified with a compliation of an order of magnitude more KBOs; neither model can be refuted by the observations available to date at a statistically significant level. With a larger database, this model can also be improved by adding a changing size distribution and/or improved phase space distribution.

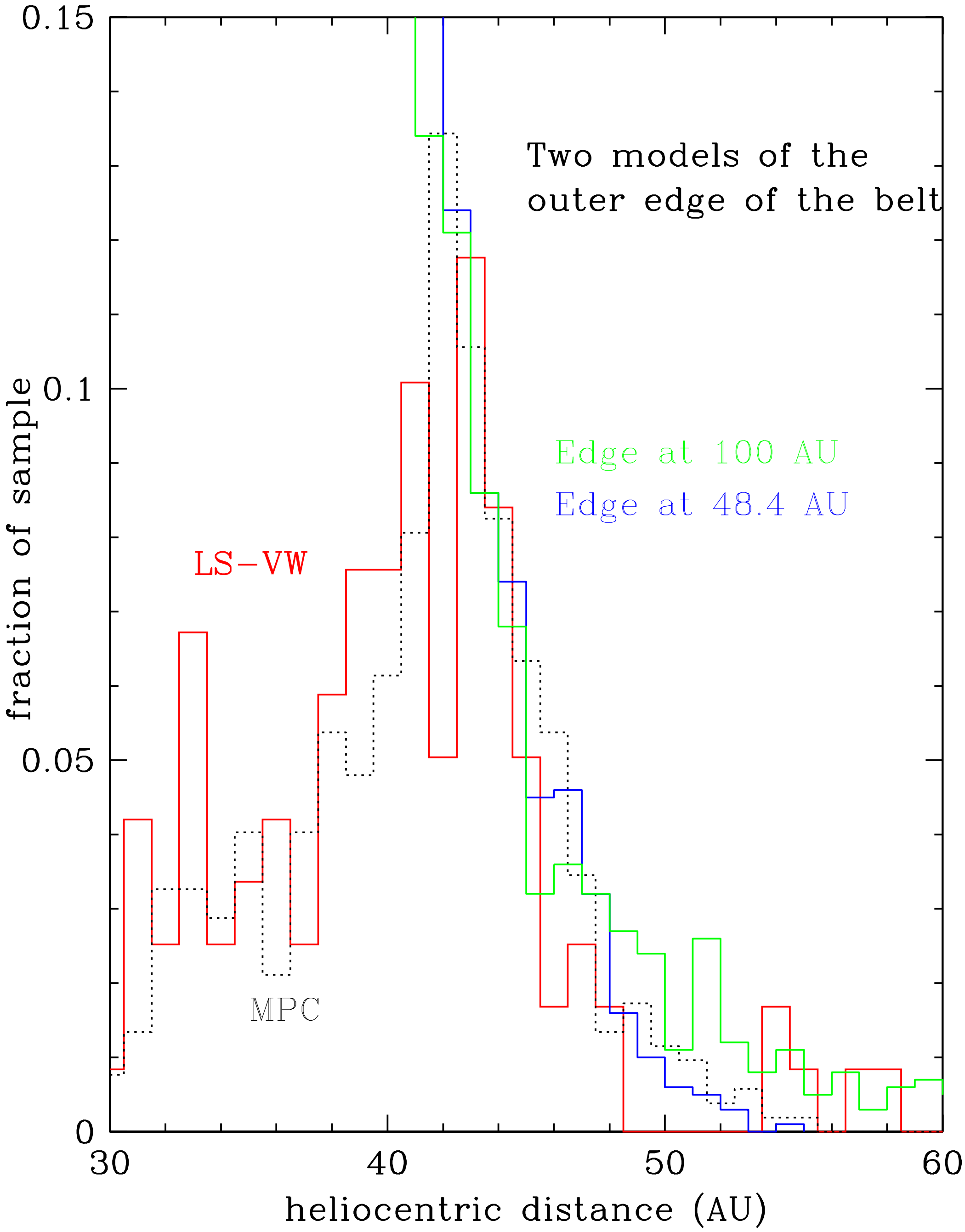

Figure 9: The distance distribution of detections in the LS-VW survey and the MPC database (red and black histograms). The Kolmogorov-Smirnov probability (using Kuiper's modified test) that these two samples are the same is 4 percent. Two models are shown of the outer edge of the belt (see text); the LS-VW distance distribution cannot reject either of them due to the lack of the very rare objects outside the 2:1 resonance at 48.4 AU (<5 percent of our detections). Vastly increased numbers of objects are needed.

A.4.2 Pericenter distribution of the scattered disk

The goal of the Canada-France ecliptic survey (CFEPS) has been to provide the community with a well-characterized survey which can be modelled by anyone wishing to do so. With a theoretical model of the Kuiper Belt's orbital and size distribution a theoretician can simulate what CFEPS should have seen if their orbital model is correct, and then refine the orbital model to improve the agreement. The parameter space of models is huge, and so only by iteration guided by physical insight can one hope to converge to the correct answer of what the outer part of our Solar System looks like.

We will illustrate this here with one example which shows the power of this approach, even if the current state of the CFEPS orbits are not enough to compare directly to a model yet.

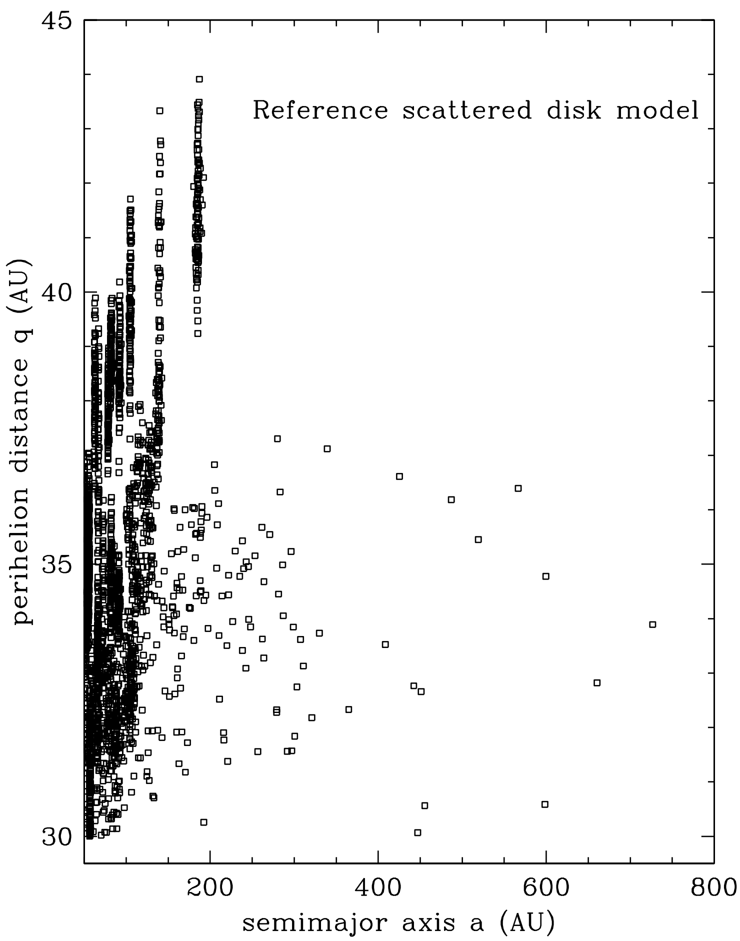

Figure 10: A numerical calcluation (see Gladman 2005) of a reference model of what the present-days scattered disk orbital distribution would be if the TNOs surviving today are simple relics of scattering off the giant planets for 4.5 Gyr. This serves as the input model to the survey simulator.

Figure 10 shows a model of the what the present day scattered disk (objects on large-semimajor axis orbits with perihelia outside of Neptune) would look if the scattered disk was created by a baseline model of Neptune scattering comets outward (see Gladman 2005 for a description of the background setting). This model is similar to the scenario of Duncan and Levison (1997), although with larger statistics. Generically one sees a scattered disk of objects with perihelia $q > 30$ but extending out to semimajor axes of hundreds of astronomical units. Some objects temporarily trapped in resonances appear as vertical features on the plot; these states are only metastable. Because the scattered disk objects spends most of their time far away from the Sun, the flux bias (which increases as distance to the fourth power because the light is reflected) against detecting the large-a objects is extreme; objects will be almost always detected near pericenter just above the flux threshold.

Fig. 11 shows the orbital elements of the simulated detections, compared to the known objects in the MPC database. As amazing as it may seen, such a plot has never been published before because of the need to have a precise knowledge of the survey circumstances. It is immediately obvious that although the known Kuiper belt objects have a semimajor axis distribution that is similar to the model, the perihelion distribution is dramatically differenct. As found by Morbidelli et al (2004), such a baseline model correctly predicts the semimajor axis and inclination distributions. However, because we have detailed knowledge of the survey parameters (magnitude limits) we can statistically prove that the perihelion distribution observed is in conflict with the observations. Fig. 12 shows the observed perihelion distribution should be biased to much smaller values; we compute a K-S probability of less than 0.01% that the detections can be drawn from model. (In contrast, without access to characterized surveys Morbidelli *et al.* were unable to prove a reliable difference between the distributions even if they recognized the possibility).

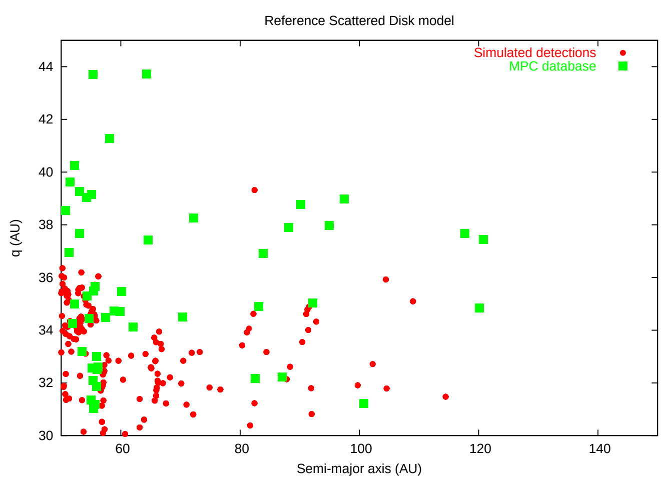

Figure 11: A comparison of the simulated detections from the survey simulator versus the Minor Planet Center's scattered disk object data base. We are unable to yet use the CFEPS orbits due to their uncertain orbital elements, but for this particular problem the MPC database shows that when flux biases are included the pericenter distribution should be too concentrated to $q < 36$ AU.

The scientific ramifications of this are dramatic. As previously concluded by Gladman et al (2001) when the scattered disk was discovered, and by Brown et al (2004) with their discovery of the distant Sedna, the outer Solar System must have somehow built a very large population of high-perihelion objects ($q > 38$ AU). This extended scattered disk is so over-abundant in the observed sample (and the analysis here makes this more extreme than previously suggested), that it is likely the most populated and massive component of the Kuiper Belt. Even with many hundreds of detections in the world-wide compliations, we know of fewer

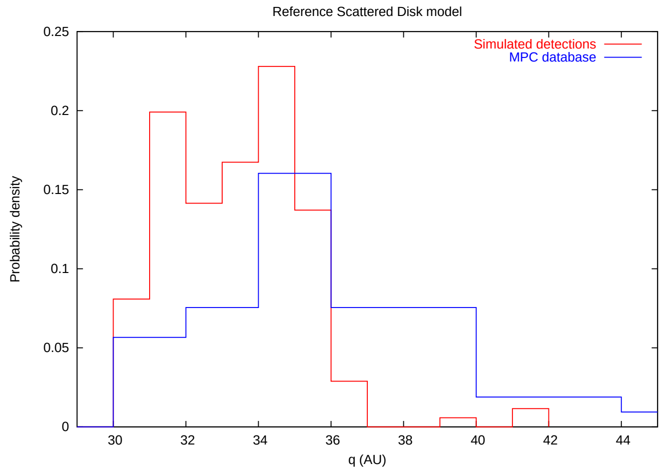

Figure 12: A histogram represenation of the pericenter distribution in the previous figure. The observations have a K-S probability of <0.1% of being drawn from this model, solidly rejecting the scenario of the scattered being only the relic of a primordial clearing of the interplanetary region. More dramatic cosmogonic scenarios are needed.

than half a dozen extended scattered disk objects. Many more detections of Kuiper Belt objects will be required to sift out these rare gems.

This kind of analysis opens a new level of enquiry into the Kuiper Belt. Theorists have been complaining for years that the compiled objects in the Minor Planet Center are impossible to de-bias since one does not know the survey parameters. Although we were forced to use the MPC database as our comparison detections here, we are able to generate a highly-significant result. This is just one example of what will be possible as soon as orbits with arcs longer than about 18 months become available from CFEPS. This will allow much more detailed models of the Kuiper Belt to be created and tested, compared to the toy power-law models in use.

REFERENCES QUOTED

Allen et al (2001) ApJL, 549, L241.

Bernstein & Khushalani (2000) AJ, 120, 3323.

Brown et al (2004) Ap. J. 617, 645.

Chiang et al (2003) AJ, 126, 430.

Duncan and Levison (1997) Science, 276, 1670.

Gladman (2005) Science, 307, 71.

Gladman et al (2002) Icarus, 157, 269.

Morbidelli et al (2004) MNRAS, 355, 935.

Trujillo & Brown (2001) ApJL, 554, L95.

B Details on the GRB program

B.1 Goals of the GRB-RTAS.

The goal of the real time analysis system (hereafter RTAS) is to quickly identify GRB afterglow candidates in the images of the sky recorded for the Very Wide (hereafter VW) survey of the CFHTLS.

Gamma-ray bursts are associated with powerful supernovae explosions leading to the ejection of ultra-relativistic material in a jet directed towards us. In the standard picture the high-energy burst is produced by mildly relativistic shocks within the jet, while the afterglow is produced by the shock of the jet on the medium surrounding the source. The dynamics and the visibility of these two components are distinct and we observe bright GRBs with faint afterglows as well as faint GRBs with bright afterglows. This standard picture also predicts the existence of 'orphan afterglows' (afterglows which are not preceded by a high-energy burst), observed when the observer's line of sight does not cross the highly-relativistic jet.

To this date, all GRB afterglows have been identified after the detection and localization of the high-energy emission, leading to important biases in the study of these events. By using the images taken for the CFHTLS VW survey we attempt the first detection of a GRB afterglow directly by its optical emission. A detection would certainly have a strong impact on future GRB studies, while no detection would provide significant constraints on the geometry and opening angles of GRB jets. Near real time operation is essential in order to confirm the GRB nature of the detections with follow-up studies while the afterglow candidate is still bright.

B.2 Operation and performance of the RTAS.

B.2.1 History

The RTAS has been accepted in March 2003, and funded by the Observatoire Midi-Pyrnes in June of the same year. The installation of the computer at the CFHT was completed in August 2003, and the first operations started in November of 2003. After these first operations it took us one year to tune the parameters for the effective detection of variable objects and rejection of false alarms. The correct balance between these two demands was reached during the summer of 2004, and since run 04BQ04 (November 2004) all the images have been checked for the presence of transient objects within 24-48 hours of their acquisition at CFHT. The developement of the software needed to search the afterglows in the images is under the responsibility of Frederic Malacrino, a PhD student at the Observatoire Midi-Pyrnes. Since the beginning of the project we benefited from an excellent support from K. Withington and J-C. Cuillandre at the CFHT.

B.2.2 Operations

Curiously, the pre-defined strategy adopted for the VW survey is well adapted for the search of GRB afterglows. The RTAS is designed to look for variable objects in images of the same field taken a few hours to a few days apart. The automatic processing includes the following steps:

- As soon as an image is released to the RTAS: construction of a catalog of astronomical objects in the image, including astrometry and photometry based on a comparison with the USNO catalog. This takes approximately 5 minutes per image.
- At the end of each night:
- Comparison of the catalogs of the same field, with the extraction of asteroids and variable objects. This takes approximately 3 minutes by comparison.
- Construction of web pages displaying asteroids and interesting variable objects.

The automatic processing results in the detection of nearly 1300000 objects per run, the identification of a few thousand asteroids, and of about 1000 variable sources. The web pages are then interpreted by a human on the same day.

B.2.3 Sensitivity

Quantitative predictions for the detection rate of orphan (and normal) GRB afterglows have been made by Totani and Panaitescu (2002). Their computations show that at any time an instrument reaching magnitude R=23 can see 300 GRB afterglows in the whole sky. Condidering the imaging of 15-20 fields per run for the Very Wide survey, we estimate the probability to find a GRB afterglow in one run to be p=(0.9*15*300)/41253=0.1 (or about 1 per year). This estimate is uncertain by a factor 3 to 5, and it is one of our goals to reduce the uncertainty. Our conclusion is that the survey has the sensitivity to detect GRB afterglows, but may fall a little bit short in terms of sky coverage. In any case we are not aware of another survey reaching the same depth over a comparable number of square degrees.

B.2.4 First results

To this date, 4 runs have been analyzed in real-time (04BQ04, 04BQ05, 04BQ06, 05AQ01), and we have found no afterglow candidate. This is consistent with the expected rate. One rapidly fading source (2.5 mag in 2 hours) was detected in run 04BQ06 and publicized in GCN 2964 (Malacrino et al.). It then appeared that the source was marginally detected in the J Band of the 2MASS survey and was most probably a flaring M star (Price GCN 2965). On the positive side we have found two GRBs which fortuitously occurred very close spatially and temporally to VW observations:

- GRB 040912 occurred at 14h12m17s UT on September 12, 2004 at RA = 23h56m54s, Dec = -1d00'02" (J2000) This is about 43 hours before exposure 761667, and only 1 degree off.
- GRB 050209 occurred at 01h31m41s UT on February 9, 2005 at RA = 08h26m09s, DEC = +19d41m02s (J2000)

This is about 31 hours before exposure 780272 and only 5 degrees off. These two 'missed shots' confirm us in the opinion that the VW survey has the right sky coverage for our purpose.

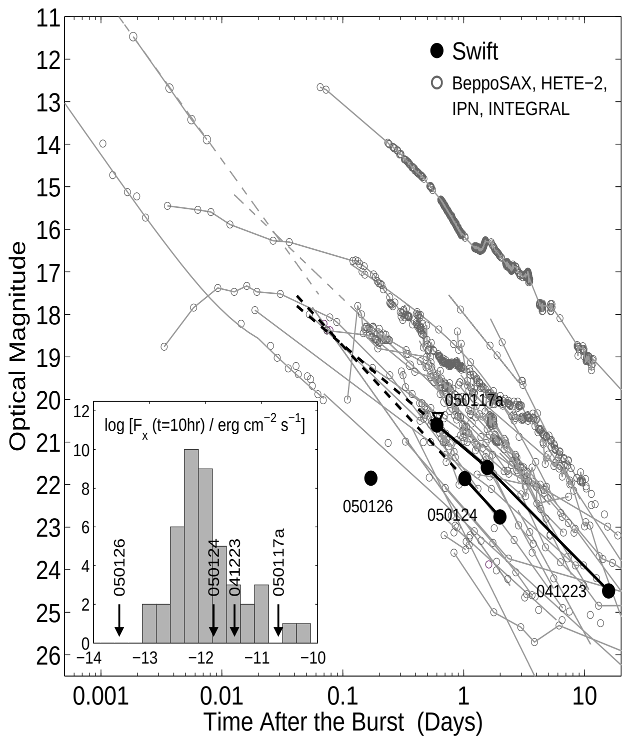

Figure 13: [Taken from Berger et al. (2005)] displays the light curves in R band of all GRB afterglows detected to date. The equivalent sensitivity of R=23 reached by our search in the images of the VW survey allows the detection of ALL GRB afterglows in the figure during one day after a burst, and the detection of more than 50% of the afterglows during 3-4 days after a burst.

B.3 Perspectives

In the coming months/years real time operations will continue. A paper describing the RTAS is now in preparation, and we are in the process of re-analysing all the data recorded to date in order to build a database of variable objects found with our analysis. This database will allow us to study the variability of the sky in a parameter space not explored to date and to provide significant constraints on the frequency of optical afterglows, independent of the gamma-ray signal.

B.4 References

RTAS web page /http://www.cfht.hawaii.edu/ grb/
Catalog page /http://www.cfht.hawaii.edu/ grb/single.html
Comparison of same night images /http://www.cfht.hawaii.edu/ grb/triple.html
Comparison of images from different nights (usually in the same run) /http://www.cfht.hawaii.edu/ grb/double.htm
Berger, E., Fox, D.B., Kulkarni, S.R. et al., 2005, ApJ, submitted (astro-ph/0502468)
Totani, T., and Panaitescu, A., 2002, ApJ, 576, 120

C QUASARS

C.1 Introduction

Observations of the cosmic microwave background and the most distant quasars have revealed the epoch of reionization and the end of the dark ages. At redshifts between z 15 and z 6 the first sources of ionizing radiation turned on and generated sufficient ionizing photons to reionize the universe. Understanding these early phases of galaxy and black hole formation are key.

Studies of the CMB and quasar spectra provide complementary probes of the reionization history. Temperature and polarization anisotropies of the CMB are most strongly dependent upon the early stages of reionization when the first free electrons appear. Lyman photons, on the other hand, are easily absorbed by even a small fraction of neutral hydrogen, so studies of quasar spectra probe the final stages of reionization.

Despite recent advances, there is still much uncertainty about exactly when the universe was reionized, whether multiple reionizations occurred and what were the sources that provided the ionizing flux. Multiple reionizations could have occurred if the initial reionization at z 15 was due to Pop III stars (extremely low metallicity) which have a higher efficiency for UV radiation than the Pop II stars which would have formed later from enriched material. Alternatively, miniquasars (black holes with masses of a few thousand solar masses which are also efficient UV producers) may have formed at z 15 and provided the source of ionizing radiation.

C.2 QUASAR surveys

Even at the lower redshift of z=6 there is uncertainty regarding both the ionization state of the universe and whether the known population of Lyman-break galaxies provide sufficient ionizing photons for reionization. The major stumbling block in understanding the late stages of reionization is the paucity of known z¿6 quasars (only 6 have so far been discovered – all by the SDSS). High-redshift galaxies are not very useful for studying the ionization state of the IGM since their UV continua are too weak for high snr spectroscopy and information based on the existence of Lyman-alpha emission lines biased by the fact the galaxies likely reside within ionized regions due to clustering. Cosmological reionization is known to be an inhomogeneous processs because underdense regions of the universe are much more easily ionized than overdense regions. Therefore many different sightlines are necessary to obtain an unbiased view of the universe.

C.2.1 A role for LS-VW

The CFHTLS is a step beyond the SDSS with deeper images of higher quality. The CFHTLS-VW goes 2 magnitudes deeper than the SDSS and covers a very large area. It is ideal for a large quasar survey. Since the CFHTLS-VW only takes observations in the g',r' and i' filters we are using MegaCam to obtain z'-band imaging of the CFHTLS-VW survey region which is covered at i'-band. i'-z' colour selection is a very efficient method for discovering high-redshift quasars as has been shown by the SDSS. Our z'-band survey will be carried out over three years (in collaboration with the brown dwarf project of X. Delfosse,

T. Forveille, et al.) and the data is to be made available to the Canadian and French communities in the same manner as the CFHTLS data. Time has already been allocated for this project in 05A.

Although the slope of the z=6 quasar luminosity function is presently highly uncertain because of the limited magnitude range of the SDSS quasars, we use extrapolation from the SDSS and constraints from a search for quasars in the CFHTLS-Deep (Willott et al. in prep.) as our best guess at the number of quasars we will discover. For a survey covering 900 sq deg, we expect somewhere in the range of 30-150 quasars at z¿5.7. Compared to the 30 z¿5.7 quasars that the SDSS will discover, it is clear that our survey will find at least as many as the SDSS and quite possibly a much larger number. Our sample will provide many high-redshift targets for reionization, host galaxy and star-formation studies with 8-10m telescopes, JWST, ALMA and SCUBA-2.

A particularly exciting development has been the novel techniques that have recently been developed to analyse quasar spectra to probe the ionization state of the universe in light of the fact that the detection of a Gunn-Peterson (G-P) trough only places a weak limit on the fraction of neutral hydrogen. Although there is not space here to fully discuss these new techniques, analyses such as the sizes of the quasar Stromgren spheres and a statistical search for ionized regions visible as gaps in the G-P trough require large samples of quasar spectra at lower snr than the traditional G-P measurements – perfect for the quasars from our survey. Other analyses to be performed are a comparison of the Lyman-alpha and Lyman-beta absorption spectra and, with future radio facilities, 21cm observations around quasars.

To advance our understanding of the ionization state of the IGM at z¿6 it is crucial that we identify a large sample of high-redshift quasars. The CFHTLS and MegaCam offer the most competitive opportunity to carry out such a survey. It is essential that the CFHTLS-VW continues to take observations in the i'-band to carry out this project.

D Brown Dwarfs

We are using the VW component of the CFHTLS to search for brown dwarfs, to a) find significantly cooler brown dwarfs than currently known, b) identify sufficient numbers of brown dwarf stars to study their spatial distribution and luminosity function, and c) to better sample the temperature/gravity plane for the 800-1200K T-dwarfs. Our brown dwarf survey will identify several thousand brown dwarfs, and accurately determine their luminosity function in the galactic disk. The large volume probed will also allow the discovery of many ultracool brown dwarfs, and could push the temperature of the coolest known brown dwarfs down by 200 K, at which point the atmospheric models predict a qualitative change in spectra, from methane-dominated (T-dwarfs) to ammonia-dominated (Y-dwarfs).

The main advantages of the VW survey (compared with the Deep and Wide) are a larger sampling volume and that the detected Brown Dwarfs are sufficiently for spectroscopic follow-up and characterisation.

Our program, however, absolutely needs i data, for a substantial fraction of the planned coverage of the VW survey and within reasonable delays. We are therefore highly concerned by a possible downgrading of the i-filter observations to lower priority, since our program only use that filter and has no use for g and r. We have hired a graduate student based on the original plan (with the expectation that any slowdown in the survey would be equally shared between filters), and his PhD would be in trouble if those plans were to now change.

We select Brown Dwarfs by their red i-z' colours, since those filters are by far the deepest for these ultra-cool objects. Furthermore, i-z' colour is an excellent spectral type estimator for brown dwarfs. The only object with $i'-z'$ redder than 1.5 are Quasars at redshifts $5.7 < z < 6.4$ (because of the sudden drop in flux shortward of the Lyman-α line) and Brown Dwarfs cooler than spectral type L0. This two object types are easily distinguished with additionanl near-infrared (J-band) observations, since quasars have blue $z' - J$ colours and Brown Dwarfs have very red $z' - J$ colours.

We have requested time from the french (I'm the PI of the french proposal) and canadian (C.Willott is the PI of this proposal) TACs to obtain z' observations of the Very Wide fields. The proposals regroup people interested by brown dwarfs and by high redshift quasar. We have obtained time on the canadian side (in fact this is the highest ranked canadian proposal for MegaCam in 2005A), and we have been given indications that the french TAC will follow suit once it gets back the 4 extra nights given to the CFHTLS in 2004B/2005A. We expect to to detect 200 T dwarfs and to find the ammonia brown dwarfs (Y-dwarfs).

Since brown dwarfs are so red, a selection using r instead of i (either with r-z or r-i) would sample a volume that is over an order of magnitude smaller. That makes such a search less sensitive than the on-going analysis of the Sloan survey, and not sufficiently interesting to justify the effort. Without i band observation for most of the survey, the CFHTLS VW would therefore not contribute to this topic